Mol Divers (2011) 15:347–360
DOI 10.1007/s11030-010-9285-y

FULL-LENGTH PAPER

Design, synthesis and activity evaluation of mannose-based DC-SIGN antagonists

Nataša Obermajer · Sara Sattin · Cinzia Colombo · Michela Bruno · Urban Švajger · Marko Anderluh · Anna Bernardi

Received: 31 May 2010 / Accepted: 18 October 2010 / Published online: 14 November 2010

Abstract In this article, we describe the design, synthesis and activity evaluation of glycomimetic DC-SIGN antagonists, that use a mannose residue to anchor to the protein carbohydrate recognition domain (CRD). The molecules were designed from the structure of the known pseudo-mannobioside antagonist **1**, by including additional hydrophobic groups, which were expected to engage lipophilic areas of DC-SIGN CRD. The results demonstrate that the synthesized compounds potently inhibit DC-SIGN-mediated adhesion to mannan coated plates. Additionally, in silico docking studies were performed to rationalize the results and to suggest further optimization.

Keywords Anti-infectives · Carbohydrates · DC-SIGN · Dendritic cell-based assay · Glycoconjugates · Glycomimetics

Abbreviations

BSA	Bovine serum albumin
CFSE	Carboxyfluorescein succinimidyl ester
CRD	Carbohydrate- recognition domain
DC	Dendritic cell
DCC	Dicyclohexyl carbodiimide
DC-SIGN	Dendritic cell-specific intercellular adhesion molecule 3-grabbing nonintegrin
DMA	*N,N*-Dimethylacetamide
DMAP	4-Dimethylaminopyridine
DMSO	Dimethyl sulfoxide
EDC	1-Ethyl-3-(3-dimethylaminopropyl)-carbodiimide
FBS	Fetal bovine serum
HATU	*O*-(7-Azabenzotriazole)- *N,N,N′,N′*-tetramethyluronium hexafluorophosphate
LPS	Lipopolysaccharide
MCPBA	*m*-Chloroperoxybenzoic acid
PAMPs	Pathogen-associated molecular patterns
PBS	Phosphate buffered saline
PFP	Pentafluorophenyl
rhGM-CSF	Recombinant human granulocyte-macrophage colony-stimulating factor
rhIL-4	Recombinant human interleukin-4
RMSD	Root mean square deviation
SAR	Structure–activity relationship
SDS	Sodium dodecyl sulfate
SPR	Surface-plasmon resonance
THF	Tetrahydrofuran
TLC	Thin-layer chromatography

Electronic supplementary material The online version of this article (doi:10.1007/s11030-010-9285-y) contains supplementary material, which is available to authorized users.

N. Obermajer
Department of Biotechnology, Jozef Stefan Institute, Jamova 39, 1000 Ljubljana, Slovenia

N. Obermajer
Department of Pharmaceutical Biology, Faculty of Pharmacy, University of Ljubljana, Aškerčeva 7, 1000 Ljubljana, Slovenia

S. Sattin · C. Colombo · M. Bruno · A. Bernardi (✉)
Dipartimento di Chimica Organica e Industriale and CISI, Università degli Studi di Milano, via Venezian 21, 20133 Milano, Italy
e-mail: anna.bernardi@unimi.it

U. Švajger
Blood Transfusion Center of Slovenia, Šlajmerjeva 6, 1000 Ljubljana, Slovenia

M. Anderluh (✉)
Department of Medicinal Chemistry, Faculty of Pharmacy, University of Ljubljana, Aškerčeva 7, 1000 Ljubljana, Slovenia
e-mail: marko.anderluh@ffa.uni-lj.si

TLR	Toll-like receptor
ManLAM	Mannosylated lipoarabinomannan
TMSOTf	Trimethylsilyl triflate

Introduction

Immature dendritic cells (DC) are the first-line guard against various pathogens that invade peripheral tissues. On binding the pathogen, they differentiate to mature DC that present antigen particles to T cells [1]. DC-SIGN (Dendritic Cell-Specific Intercellular adhesion molecule 3-Grabbing Non-integrin), a specific C-type lectin recognizing pathogen-cell surface glycoproteins, is probably the first transmembrane receptor on immature DCs that encounters invading pathogens and binds a vast number of diverse pathogen-associated molecular patterns (PAMPs). Normally, this binding event triggers internalization of the DC-SIGN-pathogen complex followed by pathogen lysosomal degradation and conjugation of the resulting fragments with MHC-II to initiate an adaptive immune response from T cells. Additionally, DC-SIGN serves as a signalling receptor that mediates pathogen-induced Toll-like receptor (TLR) signalling, which in turn modifies DC maturation and, therefore, the intensity of the adaptive immune response [2–5].

Some pathogens, however, have been reported to take advantage of this mechanism as they appear to deter DC maturation through DC-SIGN-mediated signalling and inhibit antigen presentation to T cells [6]. The van Kooyk group has shown that HIV-1 enters DC via DC-SIGN avoiding lytic degradation [7–9]. By doing so, HIV-1 not only escapes the host immune system, but also is presented directly to T cells which enables fully disseminated HIV-1 infection. Other pathogens are also believed to use the same principle for host invasion [10]. Thus, inhibition of pathogen interaction with DC-SIGN specific antagonists is considered as a plausible concept for new anti-infective agents. Several groups have recently demonstrated that inhibition of DC-SIGN, either by designed glycoconjugates or by antibodies, prevents pathogen attachment to DC and inhibits the infection of other immune cells at its earliest steps [11–23]

DC-SIGN specifically binds mannose and fucose-glycosylated endogenous proteins (ICAM-2 and -3) as well as mannosylated PAMPs (HIV-1 gp120, *M. tuberculosis* ManLAM and others) [7,9]. Moreover, mannose- and fucose-containing oligosaccharides (such as Lewis-x) bind to DC-SIGN with moderate to high affinity, while both Man and Fuc themselves have only weak affinity [24]. As a consequence, glycomimetic structures designed to inhibit DC-SIGN have been based on oligomannosides or on Lewis-x. In our previous study, we concentrated on the design and synthesis of monovalent glycoconjugates as glycomimetic DC-SIGN antagonists [12,15,21]. These molecules (Fig. 1, **1–3**) have been conceived to be metabolically more stable than native oligosaccharides and/or equipped with reactive moieties to enable their multimeric presentation on multivalent supports. Ligands **1–3** had moderate to weak affinities for DC-SIGN, comparable or slightly superior to those of the starting oligosaccharide templates [12,15,21]. Thereby they displayed only limited therapeutic potential in their monomeric form. However, when presented in multimeric form, they were effective inhibitors of DC-SIGN-mediated viral infection. Indeed, the pseudo-trisaccharide **2**, mimicking a linear Man-α-1,2-Man-α-1,6-trimannoside was found to inhibit DC-SIGN binding to mannosylated BSA with an IC_{50} of 130 μM (by surface-plasmon resonance—SPR) and, when presented on a tetravalent dendron, was also found to inhibit the *trans* infection of CD4+T lymphocytes by HIV at low micromolar concentrations [21].

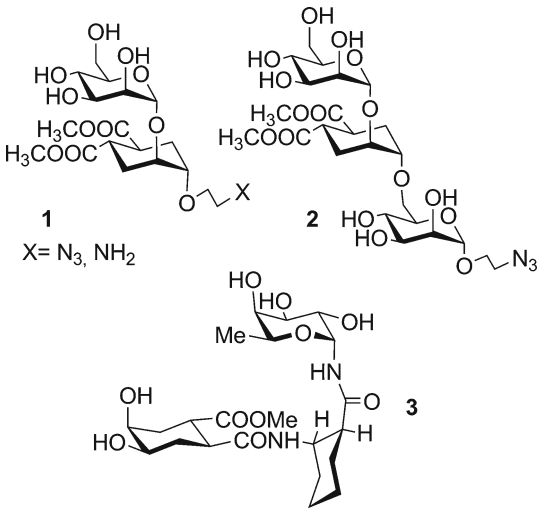

Fig. 1 Previously reported glycomimetic DC-SIGN antagonists: the mannose-based ligands **1** and **2** and the fucose-based ligand **3**

To improve binding affinities of monovalent glycoconjugates, we have now designed mannose-based glycoconjugates derived from **1** which could bind into new binding areas of DC-SIGN carbohydrate recognition domain (CRD), that are not occupied by the native ligands. Ligand candidates were synthesized and their affinity to DC-SIGN was evaluated by an in vitro assay that measures inhibition of DC-SIGN-mediated immature dendritic cell adhesion to mannan-coated plates [25]. Additionally, docking studies were performed to rationalize the results and to suggest further optimization. Assay data demonstrate that our effort to design and synthesize mannose-based DC-SIGN antagonists has resulted in compounds which potently inhibit DC-SIGN-mediated adhesion to mannan-coated plates and have the potential to prevent DC-SIGN-mediated pathogen recognition by DC.

Table 1 Structure of compounds **16–50**

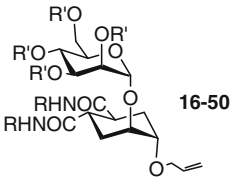

R′ = Bz	R′ = H	R =	R′ = Bz	R′ = H	R =
16	26		24	35	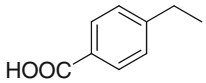
17	27	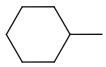	25	36	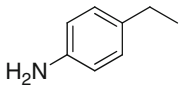
18	28	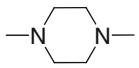	37	44	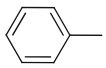
19	29	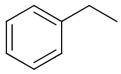	38	45	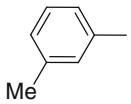
20	30	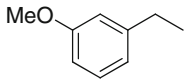	39	46	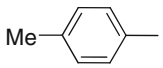
21	31	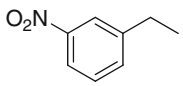	40	47	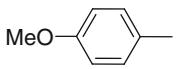
22	32	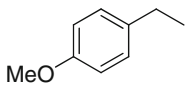	41	48	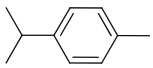
23	33	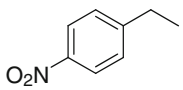	42	49	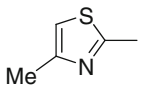
24	34	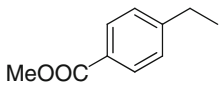	43	50	

Experimental

In Silico Molecular docking studies

Ligand preparation

The molecules (Table 1) were built with ChemBioDraw Ultra 12.0 [26]. The ligand geometries were optimized with ChemBio 3D Ultra 12.0 using MM2 force field until a minimum 0.100 RMS gradient was reached [26]. The optimized structure was refined with GAMESS interface using the semi-empirical AM1 method, QA optimization algorithm and Gasteiger Hückel charges for all atoms for 100 steps [27]. The carboxylate (**35**) and non-aromatic amine (**28**) were kept in their ionized state at to pH 7.4.

Receptor preparation and docking protocol

The crystal structure of DC-SIGN CRD (chain A; 131 amino-acid sequence) in complex with Man_4 (PDB code 1SL4) [28] was taken as a starting-point. The ligand Man_4 was taken as a reference structure and an area of 14 Å around it was considered as the active site. The crystal structure was cleaned with FlexX 3.1.2 [29] by deleting the ligand (Man_4) and crystallographic water molecules. Hydrogens were automatically added to all heavy atoms. Two water molecules (HOH residues 512 and 519; 152 and 105 in FlexX) were preserved as 'freely rotatable water' in docking studies since one (519 – FlexX ID: 105) stabilizes interactions between Man1 residue and the receptor while the other one (512—FlexX ID: 152) stabilizes the Man_4 binding conformation.

Additionally, PharmMetal pharmacophore with spherical coordination around Ca^{2+} was defined to correctly account for complex interactions between Ca^{2+} (406) and Man1 residue. The side-chains of aspartate, glutamate, lysine and arginine residues were kept in their ionized state at to pH 7.4.

The FlexX 3.1.2 molecular docking program for structure-based design was used for ligand docking using the standard triangle algorithm to place the 'base fragment'. The parameters in FlexX modified/optimized for the docking studies were: (a) clash handling, (b) maximum number of solutions per iteration and (c) maximum number of solutions per fragmentation. The proposed 10 binding modes with the highest rank of the docked antagonists were evaluated using final score and RMSD as a tool to explore relative structural differences between proposed binding modes. The graphical representations of the proposed binding positions of molecules **26–36** and **44–50** were obtained using Accelrys Discovery Studio 2.5. [30].

Validation of the docking protocol

The docking procedure should be able to correctly predict the binding orientation of the molecules in the PDB database, i.e. the crystal structures of ligands in complex with proteins. We have attempted to reproduce the pose of Man_4 as seen in its X-ray complex with the target DC-SIGN CRD (1SL4) [28]. The top 10 docking poses were within 1.5 Å root mean square deviation (RMSD) of the crystal structure for Man1 and Man2 residues of Man_4. The predicted top score pose was the one that best fitted the crystal structure of Man_4 overlapping reasonably well (Fig. 2).

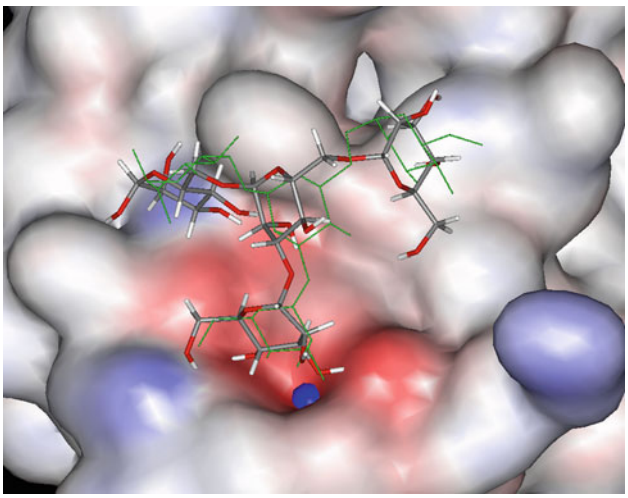

Fig. 2 Crystal structure of DC-SIGN CRD (shown as solvent-accessible surface; Ca^{2+} coordinated by Man1 residue is presented as a sphere) in complex with Man_4 (shown as lines) and top-docked pose (shown as tubes)

Synthesis

General

Dichloromethane, methanol, *N,N*-diisopropylethylamine and triethylamine were dried over calcium hydride; THF was distilled over sodium, *N,N*-dimethylacetamide (DMA) was dried over activated molecular sieves. Reactions requiring anhydrous conditions were performed under nitrogen. ^{1}H, ^{13}C and ^{19}F-NMR spectra were recorded at 400 MHz on a Bruker AVANCE-400 instrument. Chemical shifts (δ) for ^{1}H and ^{13}C spectra are expressed in ppm relative to internal Me_4Si as standard. Signals were abbreviated as s, singlet; bs, broad singlet; d, doublet; t, triplet; q, quartet; m, multiplet. Sugar signals were numbered as customary; cyclohexane protons are indicated with the letter D followed by numbers. Numbering of the cyclohexane ring in compounds **10–50** is unconventional (see Figure SI-1 in the Supplementary Information file) and it was adopted to facilitate comparison with the native disaccharide. Mass spectra were obtained with a ThermoFisher LCQ apparatus (ESI ionization), or ion-trap ESI Esquire 6000 from Bruker, or a Microflex apparatus (MALDI ionization) from Bruker, or Apex II ICR FTMS (ESI ionization—HR-MS). Specific optical rotation values were measured using a Perkin-Elmer 241, at 589 nm, in a 1 dm cell. Thin layer chromatography (TLC) was carried out with pre-coated Merck F_{254} silica gel plates. Flash chromatography (FC) was carried out with Macherey-Nagel silica gel 60 (230–400 mesh). Compounds **12** [31] and **5** [32] have been described. The synthesis of **6–13** and the general procedures for the synthesis of amides **16–36** and anilides **37–50** are described. The characterization of compounds **16–50** is reported in Supplementary Information.

(1S,2S)-4-Cyclohexen-1,2-dicarboxylic acid bis-pentafluorophenylester **6**

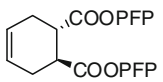

EDC·HCl (743 mg, 3.877 mmol, 3.3 eq.) was added to a solution of the diacid **5** [32] (200 mg, 1.175 mmol, 1 eq.) in dry THF (11 mL) under stirring and under a nitrogen atmosphere. After 10 min pentafluorophenol (649 mg, 3.525 mmol, 3 eq.) was added. The solution was stirred at room temperature for 2 h. After completion of the reaction the solvent was evaporated under reduced pressure, the residue was dissolved in Et_2O, the organic phase washed with 1M HCl and saturated Na_2CO_3, then dried over sodium sulphate. Solvent was evaporated under reduced pressure yielding 519 mg (yield = 88%) of pure **6** as a colourless oil.

$[\alpha]_D^{20} = +53.6$ ($c = 0.5$; $CHCl_3$). **^{1}H-NMR (400 MHz, $CDCl_3$)**: 5.81 (app d, $J = 2.68$ Hz, 2H, H_4, H_5), 3.40–3.31 (m, 2H, H_1, H_2), 2.80–2.68 (m, 2H, $H_{3ps\text{-}eq}$, $H_{6ps\text{-}eq}$), 2.50–2.38 (m, 2H, $H_{3ps\text{-}ax}$, $H_{6ps\text{-}ax}$).[13] **^{13}C-NMR (100 MHz, $CDCl_3$)**: 170.5 (**COOPFP**); 142.6 (m, CF); 141.2 (m, CF); 140.1 (m, CF); 139.4 (m, CF); 138.7 (m, CF); 136.9 (m, CF); 124.7 (C_4, C_5); 40.8 (C_1, C_2); 27.8 (C_3, C_6). **^{19}F-NMR (282 MHz, $CDCl_3$)**: −153.2 (d, 2F, F_{ortho}, $J_{o\text{-}m} = 20$ Hz), −157.9 (t, 1F, F_{para}, $J_{p\text{-}m} = 22.5$ Hz), −162.4 (t, 2F, F_{meta}).

*Epoxide of the (1S,2S)-4-cyclohexen-1,2-dicarboxylic acid bis-pentafluorophenyl ester **8***

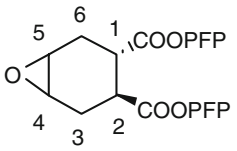

77% MCPBA was added (385 mg, 1.8 mmol, 1.4 eq.) to a solution of the PFP ester **6** (660 mg, 1.3 mmol, 1 eq.) in dry CH_2Cl_2 (4.4 mL) under stirring. The reaction was stirred under nitrogen at room temperature until TLC (8:2 Hexane:EtOAc) showed disappearance of the starting material. The solvent was evaporated at reduced pressure, the reaction mixture was diluted with EtOAc and washed with saturated $NaHCO_3$ and with water. The organic phase was dried over sodium sulphate and the solvent evaporated under reduced pressure, yielding 636 mg of crude product that was purified by flash chromatography (8:2 Hex:EtOAc) affording 533 mg (78%) of pure **8**.

$[\alpha]_D^{20} = +37.7$ ($c = 0.5$; $CHCl_3$). **MS (FAB)** calculated for $[C_{20}H_9F_{10}O_5]^+$: 519; found: 519. **^{1}H-NMR (400 MHz, $CDCl_3$)**: 3.43–3.34 (m, 2H, H_4 or H_5, H_2 or H_1), 3.32 (dd, 1H, H_5 or H_4, $J_{5\text{-}4} = J_{5\text{-}6}$ or $J_{4\text{-}3} = 4$ Hz), 3.14 (dt, 1H, H_2 or H_1, $J_{2\text{-}3eq}$ or $J_{1\text{-}6eq} = 6.8$ Hz, $J_{2\text{-}3ax}$ or $J_{1\text{-}6ax} = J_{2\text{-}1} = 10.0$ Hz), 2.76 (ddd, 1H, H_{3eq}o H_{6eq}, $J_{3eq\text{-}4}$ or $J_{6eq\text{-}5} = 1.6$ Hz, $J_{3eq\text{-}2}$ or $J_{6eq\text{-}1} = 5.2$ Hz, $J_{gem} = 14.8$ Hz), 2.61 (ddd, 1H, H_{6eq} or H_{3eq}, $J_{6eq\text{-}1}$ or $J_{3eq\text{-}2} = 4.4$ Hz, $J_{gem} = 15.6$ Hz), 2.37 (dd, 1H, H_{6ax} or H_{3ax}), 2.16 (ddd, 1H, H_{3ax} or H_{6ax}, $J_{3ax\text{-}4}$ or $J_{6ax\text{-}5} = 2.0$ Hz). **^{13}C-NMR (100 MHz, $CDCl_3$)** :170.6, 169.4 (CO_{PFP}); 142.6 (m, CF); 141.1 (m, CF); 140.0 (m, CF); 139.4 (m, CF); 138.7 (m, CF); 137.3 (m, CF); 51.5, 50.1 (C_4, C_5); 39.4, 37.5 (C_1, C_2); 26.9, 26.2 (C_3, C_6).

*(1S,2S,4S,5S)-4-allyloxy-5-hydroxy-cyclohexan-1,2-bispentafluorophenylester **10***

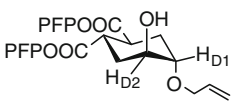

Allylic alcohol (2 mL, 27.32 mmol, 30 eq.) and $Cu(OTf)_2$ (33 mg, 0.09 mmol, 0.1 eq.) were added to a solution of the epoxide **8** (472 mg, 0.91 mmol, 1 eq.) in the minimum amount of dry CH_2Cl_2 (334 μL) under stirring and under nitrogen. The solution was stirred at room temperature. After completion (ca. 4 h; TLC 9:1 toluene:EtOAc) the reaction mixture was directly purified by flash chromatography (95:5 toluene:EtOAc) yielding 497 mg (yield = 95%) of pure product **10** as a yellow oil.

$[\alpha]_D^{20} = +4.5$ ($c = 1.1$; $CHCl_3$) **MS (ESI)** calculated for $[C_{23}H_{14}F_{10}O_6Na]^+$: 599.1; found: 599.6. **^{1}H-NMR (400 MHz, $CDCl_3$)**: 6.00–5.90 (m, 1H, H_8), 5.34 (dd, 1H, H_{9trans}, $J_{9\text{-}9} = 1.3$ Hz, $J_{9\text{-}8trans} = 17.2$ Hz), 5.25 (dd, 1H, H_{9cis}, $J_{9\text{-}8cis} = 10.4$ Hz), 4.12 (m, 1H, H_2), 4.18 (dd, 1H, H_{7b}, $J_{7\text{-}8} = 5.2$ Hz, $J_{7\text{-}7} = 12.8$ Hz), 4.07 (dd, 1H, H_{7a}, $J_{7\text{-}8} = 4.5$ Hz), 3.64 (dd, 1H, H_1, $J_{1\text{-}2} = 4.0$ Hz, $J_{1\text{-}6ass} = 6.8$ Hz), 3.62–3.46 (m, 2H, H_4, H_5), 2.31–2.18 (m, 2H, H_6), 2.28–2.22 (m, 2H, H_3), 1.82 (d, 1H, OH, $J = 3.0$ Hz). **^{13}C-NMR (100 MHz, $CDCl_3$)** : 170.4, 170.4 (CO_{PFP}); 142.3 (m, CF); 140.9 (m, CF); 139.8 (m, CF); 139.1 (m, CF); 138.4 (m, CF); 136.6 (m, CF); 134.4 (C_8); 117.4 (C_9); 74.9 (C_1); 70.3 (C_7); 66.5 (C_2); 38.9 (C_4); 38.4 (C_5); 30.5 (C_3); 27.2 (C_6).

*Tetra-O-benzoyl α-(1,2)-pseudomannobioside bis-pentafluorophenylester **13***

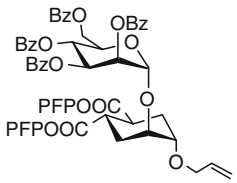

A mixture of the acceptor **10** (418 mg, 0.725 mmol, 1 eq.) and the donor **12** [31] (644 mg, 0.870 mmol, 1.2 eq.) was co-evaporated with toluene three times. Powdered acid washed 4Å molecular sieves were added; the mixture was kept under vacuum for a few hours and then dissolved with dry CH_2Cl_2 (7.25 mL). After cooling at −20 °C, TMSOTf (26 μL, 0.145 mmol, 0.2 eq.) was added to the reaction mixture under stirring. The reaction was monitored by TLC (85:15 Toluene:EtOAc, 7:3 Hexane:EtOAc) and was finished after 20 min. The reaction was quenched with Et_3N and the mixture warmed to room temperature and filtered over a celite pad. The filtrate was evaporated at reduced pressure and the crude product purified by flash chromatography (75:25 Hex:EtOAc) to yield 470 mg of **13** (56%).

MS (ESI): calculated for $[C_{57}H_{40}F_{10}O_{15}Na]^+$: 1177.2; found: 1177.3. **^{1}H-NMR (400 MHz, $CDCl_3$)**: 8.08 (d, 4H, H_{Bz}, $J = 7.4$ Hz), 8.00 (d, 2H, H_{Bz}, $J = 7.2$ Hz), 7.84 (d, 2H, H_{Bz}, $J = 7.2$ Hz), 7.66–7.50 (m, 3H, H_{Bz}), 7.49–7.34 (m, 6H, H_{Bz}), 7.34–7.23 (m, 3H, H_{Bz}), 6.11 (t, 1H,

H_4, $J_{4\text{-}3} = J_{4\text{-}5} = 10.0$ Hz), 5.99–5.87 (m, 1H, H_3), 5.92–5.87 (m, 1H, H_8), 5.78 (m, 1H, H_2), 5.33 (d, 1H, H_1, $J_{1\text{-}2} = 1.2$ Hz), 5.30 (dd, 1H, H_{9trans}, $J_{9\text{-}9} = 1.3$ Hz, $J_{9\text{-}8trans} = 17.2Hz$), 5.22 (dd, 1H, H_{9cis}, $J_{9\text{-}8cis} = 10.3$ Hz), 4.71 (dd, 1H, H_{6b}, $J_{6\text{-}5} = 2.6$ Hz, $J_{6a\text{-}6b} = 12.1$ Hz), 4.55 (dd, 1H, H_{6a}, $J_{6\text{-}5} = 4.9$ Hz), 4.47–4.44 (m, 1H, H_5), 4.21 (m, 1H, D_2), 4.11 (dd, 1H, H_{7b}, $J_{7\text{-}8} = 6.5$ Hz, $J_{7\text{-}7} = 12.8$ Hz), 4.00 (dd, 1H, H_{7a}, $J_{7\text{-}8} = 5.7$ Hz), 3.87 (m, 1H, D_1), 3.61–3.49 (m, 2H, D_4, D_5), 2.55–2.40 (m, 2H, D_{3eq}, D_{6eq}), 2.30–2.12 (m, 2H, D_{3ax}, D_{6ax}). **^{13}C-NMR (100 MHz, $CDCl_3$)**: 170.2, 170.1 (CO_{PFP}); 166.1, 165.6, 165.5, 165,4 (CO_{BZ}); 134.2 (C_8); 133.7, 133.6, 133.3, 133.2 (CH_{BZ}); 129.9, 128.9, 129.7, 129.7 (CH_{BZ}); 129.7, 129.1, 128.9, 128.8 ($Cquat_{BZ}$); 128.7, 128.5, 128.4, 128.4 (CH_{BZ}); 117.6 (C_9); 96.5 (C_1); 73.2 (C_{D1}); 72.2 (C_{D2}); 70.6 (C_2); 70.5 (C_7); 69.8 (C_3); 69.7 (C_5); 67.0 (C_4); 63.0 (C_6); 38.7, 38.6 (C_{D4}, C_{D5}); 28.0 (C_{D3}); 27.2 (C_{D6}).

*General procedure for the synthesis of amides **26–36***

The amine (2.4 eq.) was added to a 0.4 M PFP-scaffold **13** (1 eq.) in dry THF under stirring and under nitrogen atmosphere at room temperature. After completion (TLC 7:3 Hexane:EtOAc, 98:2 $CHCl_3$:MeOH) the solvent was evaporated under reduced pressure. The crude product was purified using three consecutive 3 mL Isolute H-MN columns conditioned with 1M HCl, 1M NaOH and water. Finally, it was dissolved in 5 mL of EtOAc and eluted gravimetrically. The organic phase was collected; the solvent was evaporated at reduced pressure, obtaining the pure products **16–25**. These were directly deprotected using the following general procedure: to a 0.05 M solution of the bis-amide (1 eq.) in dry methanol, under nitrogen at room temperature, a 1M solution of sodium methoxide in MeOH (2 eq.) was added. After reaction completion (TLC 96:4 and 8:2 $CHCl_3$:MeOH) the reaction mixture was diluted with methanol and neutralized with prewashed Amberlite IRA 120-H^+. The resin was filtered off and the solvent evaporated under reduced pressure. The crude was purified by flash chromatography (95:5 $CHCl_3$:MeOH).

*(1S,2S)-4-cyclohexen-1,2-dicarboxylic acid bis-(2-trimethylsilyl)-ethylester **7***

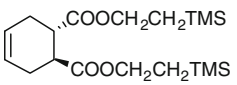

Trimethylsilylethanol (2.1 mL, 14.63 mmol, 2.2 eq.) and DMAP (56.5 mg, 0.4624 mmol, 0.05 eq.) were added to a solution of the diacid **5** [32] (1.3 g, 6.65 mmol, 1 eq.) in dry CH_2Cl_2 (9 mL) under stirring. Separately DCC (3.0 g, 14.63 mmol, 2.2 eq.) was dissolved in CH_2Cl_2 (9 mL) and the solution added dropwise to the previous one cooled at 0 °C under stirring. After 15 min the reaction mixture was warmed to room temperature and stirred for 24 h. After reaction completion (TLC 99:1 hexane:EtOAc) the reaction mixture was diluted with CH_2Cl_2 and filtered on a celite pad. The solvent was evaporated at reduced pressure. The product was purified by flash chromatography (95:5 hexane:EtOAc) obtaining 2.12 g (yield = 86%) of pure **7**.

$[\alpha]_D^{20} = +66.5$ ($c = 1.2$; $CHCl_3$). **LC-MS** (**ESI**) calculated for $[C_{18}H_{34}O_4Si_2Na]^+$: 393.63; found: 393.20. **^{1}H-NMR(400MHz, $CDCl_3$)** : 5.72–5.66 (m, 2H, H_4, H_5), 4.23–4.14 (m, 4H, H_7), 2.87–2.77 (m, 2H, H_1, H_2), 2.47–2.29 (m, 2H, H_{3psdeq}, H_{6psdeq}), 2.23–2.11 (m, 2H, H_{3psdax}, H_{6psdax}), 1.0–0.9 (m, 4H, H_8), 0.03 (s, 18H, H_9). **^{13}C-NMR (100 MHz, $CDCl_3$)**: 175.0, 173.4 (CO); 125.2, 125.0, (C_4, C_5); 62.8 (C_7); 41.3 (C_2); 39.8 (C_1); 27.9 (C_3); 25.8 (C_6); 17.3, 17.0 (C_8); −1.5 (C_9).

*Epoxide of the (1S,2S)-4-cyclohexen-1,2-dicarboxylic acid bis-(2-trimethylsilyl)-ethylester **9***

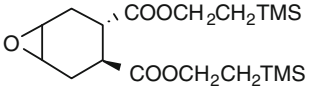

77% MCPBA was added (1.8 g, 8.00 mmol, 1.2 eq.) to a solution of the trimethylsilylethyl ester **7** (2.5 g, 6.66 mmol, 1 eq.) in dry CH_2Cl_2 (22 mL) under stirring. The reaction was stirred under nitrogen at room temperature. After completion of the reaction (2 h; TLC 95:5 toluene:EtOAc), the reaction mixture was diluted with CH_2Cl_2 and washed with saturated $NaHCO_3$ and with water. The organic phase was dried over sodium sulphate and the solvent evaporated under reduced pressure, obtaining 2.66 g of crude product that was purified by flash chromatography (9:1 hexane:EtOAc + 0.5% AcOH) yielding to 1.43 g (yield= 71%) of pure product **9**.

$[\alpha]_D^{20} = +34.5$ ($c = 1.15$; $CHCl_3$). **^{1}H-NMR(400MHz, $CDCl_3$)**: 4.14–4.09 (m, 4H, H_7), 3.23–3.19 (m, 1H, H_4), 3.21 (t, 1H, H_5, $J_{5\text{-}4} = J_{5\text{-}6psdeq} = 4$ Hz), 2.84 (dt, 1H, H_2, $J_{2\text{-}1} = J_{2\text{-}3psdax} = 10.8$ Hz, $J_{2\text{-}3psdeq} = 4.8$ Hz), 2.61 (dt, 1H, H_1, $J_{1\text{-}6psdax} = 10.4$ Hz, $J_{1\text{-}6psdeq} = 6.4$ Hz), 2.49 (ddd, 1H, H_{3psdeq}, $J_{gem} = 14.8$ Hz, $J_{3psdeq\text{-}4} = 2$ Hz), 2.33 (ddd, 1H, H_{6psdeq}, $J_{gem} = 15.2$ Hz), 2.09 (dd, 1H, H_{6psdax}), 1.92 (ddd, 1H, H_{3psdax}, $J_{3\text{-}4} = 2$ Hz), 1.03–0.95 (m, 4H, H_8), 0.07 (s, 18H, H_9). **^{13}C-NMR(100MHz, $CDCl_3$)** : 174.8 (CO); 173.9 (CO); 63.1 (C_7); 51.9 (C_4); 50.4 (C_5); 40.1 (C_1); 37.8 (C_2); 27.2 (C_3); 26.4 (C_6); 17.3 (C_8); −1.5 (C_9).

*(1S,2S,4S,5S)-4-allyloxy-5-hydroxy-cyclohexan-1,2-bis-(2-trimethylsilyl)-ethylester **11***

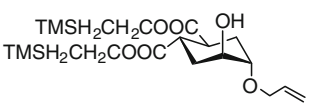

$Cu(OTf)_2$ (111.2 mg, 0.3078 mmol, 0.1 eq.) was added to a solution of the epoxide **9** (1.2 g, 3.78 mmol, 1 eq.) in allylic alcohol (6.3 mL, 92.34 mmol, 30 eq.) under stirring and under nitrogen atmosphere. The solution was stirred at room temperature. After reaction completion (5 h; TLC 95:5 toluene:EtOAc) the reaction mixture was diluted with Et_2O, washed with 1:1 NH_3: saturated NH_4Cl, then with saturated NH_4Cl. The organic phase was dried over sodium sulphate and the solvent evaporated under reduced pressure. The crude product was purified by flash chromatography (85:15 toluene:EtOAc) yielding 1.26 g (yield = 91%) of pure product **11**.

$[\alpha]_D^{20} = +11.3$ ($c = 1.04$; $CHCl_3$). **^{1}H-NMR(400 MHz, CDCl$_3$)**: 5.95–5.80 (m, 1H, H_8), 5.25 (dq, 1H, H_{9trans}, $J_{trans} = 17.2$ Hz, $J_{gem} = J_{9trans\text{-}7A} = J_{9trans\text{-}7B} = 1.6$ Hz), 5.15 (dq, 1H, H_{9A}, $J_{cis} = 12.8$ Hz, $J_{9cis\text{-}7A} = J_{9cis\text{-}7B} = 1.6$ Hz), 4.18–4.06 (m, 5H, H_{7B}, H_{10}), 3.95 (ddt, 1H, H_{7A}, $J_{gem} = 12.8$ Hz, $J_{7A\text{-}8} = 5.6$ Hz), 3.85–3.78 (m, 1H, H_2), 3.43–3.37 (m, 1H, H_1), 3.10–2.95 (m, 2H, H_4, H_5), 2.15–1.97 (m, 2H, H_{3eq}, H_{6eq}), 1.93 (d, 1H. OH, $J_{OH\text{-}H2} = 2.4$ Hz), 1.90–1.75 (m, 2H, H_{3ax}, H_{6ax}), 1.00–0.90 (m, 4H, H_{11}), 0.02 (s, 9H, H_{12}), 0.01 (s, 9H, H_{12}). **^{13}C-NMR (100 MHz, CDCl$_3$)** : 174.7, 174.6 (CO); 135.0 (C_8), 117.1 (C_9); 76.8 (C_1); 70.1 (C_7); 68.3 (C_2); 63.2, 63.2 (C_{10}); 40.0, 39.6 (C_4, C_5); 30.8 (C_3); 27.3 (C_6); 17.6, 17.6 (C_{11}); −1.3(C_{12}).

*Tetra-O-benzoyl α-(1,2)-pseudomannobioside bis-(2-trimethylsilyl)-ethylester **14***

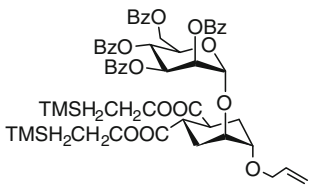

A mixture of the acceptor **11** (140 mg, 0.313 mmol, 1 eq.) and the donor **12** [31] (278 mg, 0.375 mmol, 1.2 eq.) was co-evaporated with toluene three times. Powdered acid washed 4Å molecular sieves were added. The mixture was kept under vacuum for few hours and then dissolved in dry CH_2Cl_2 (3 mL). After cooling to −20 °C, TMSOTf (11 μL, 0.0625 mmol, 0.2 eq.) was added to the reaction mixture under stirring. The reaction was stirred at that temperature and was monitored by TLC (9:1 toluene:EtOAc, 95:5 $CHCl_3$:acetone): after 30 min the reaction was quenched by adding NEt_3. The mixture was then warmed to room temperature and filtered on a celite pad. The filtrate was evaporated under reduced pressure and the product purified by flash chromatography (95:5 toluene:EtOAc) yielding 154 mg (48%) of **14**.

$[\alpha]_D^{20} = -31.0$ ($c = 1.01$; $CHCl_3$). **^{1}H-NMR(400 MHz, CDCl$_3$)** : 8.05 (d, H-Ph, $J = 5.2$ Hz), 8.00–7.90 (m, H-Ph), 7.72 (d, H-Ph, $J = 7.6$ Hz), 7.64–7.52 (m, H-Ph), 7.52–7.46 (m, H-Ph), 7.46–7.30 (m, H-Ph), 7.24 (d, H-Ph, $J = 5.2$ Hz), 6.06 (t, 1H, H_4, $J = 10$ Hz), 5.95–5.80 (m, 2H, H_3, H_8), 5.70 (bs, 1H, H_2), 5.28 (dd, 1H, H_{9B}, $J_{trans} = 18$ Hz), 5.23 (s, 1H, H_1), 5.14 (dd, 1H, H_{9A}, $J_{9A\text{-}9B} = 1.2$ Hz, $J_{cis} = 10.4$ Hz), 4.63 (d, 1H, H_{6b}, $J_{gem} = 13.6$ Hz), 4.42 (m, 2H, H_{6A}, H_5), 4.26–4.10 (m, 4H, H_{10}), 4.08 (dd, 1H, H_{7B}, $J_{gem} = 12$ Hz, $J_{7B\text{-}8} = 5.2$ Hz), 4.02–3.97 (m, 1H, D_2), 3.94 (dd, 1H, H_{7A}, $J_{7A\text{-}8} = 5.6$ Hz), 3.72–3.68 (m, 1H, D_1), 3.07–2.93 (m, 2H, D_4, D_5), 2.13–1.94 (m, 4H, D_3, D_6), 1.07–0.97 (m, 4H, H_{11}), 0.04 (s, 9H, $(CH_3)_3$-Si), 0.02 (s, 9H, $(CH_3)_3$-Si). **^{13}C-NMR(100MHz, CDCl$_3$)** : 174.7, 174.6 (CO); 166.2, 165.6, 165.5, 165.4 (CO_{BZ}); 132.9, 129.1, 127.8 (CH_{BZ}); 134.2 (C_8); 128.60, 128.46, 128.45, 128.30 (C_{quatBZ}); 116.9 (C_9); 95.0 (C_1); 73.1 (C_{D1}); 71.2 (C_{D2}); 70.2 (C_2); 69.8 (C_7); 69.3 (C_5); 69.1 (C_3); 67.7 (C_4); 63.0 (C_{10}); 62.6 (C_6); 38.6 (C_{D4}, C_{D5}); 26.8 (C_{D3}, C_{D6}); 17.4 (C_{11}); −2.0 (($CH_3)_3$-Si).

*Tetra-O-benzoyl α-(1,2)-pseudomannobioside diacid **15***

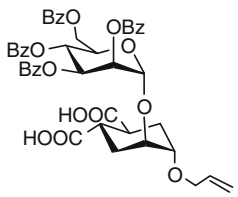

CF_3 COOH (18.5 mL) was added to a solution of the diester **14** (1.128 g, 1.103 mmol) in dry CH_2Cl_2 (18.5 mL) under stirring. The solution was stirred under nitrogen atmosphere at room temperature. After 20 min (TLC 6:4 Hex:EtOAc) the solvent was co-evaporated with toluene three times, yielding 963 mg (quantitative) of pure product **15**.

$[\alpha]_D^{20} = -31.6$ ($c = 1.01$; $CHCl_3$). **MS (MALDI-TOF, matrix DHB)**: calculated for $[C_{45}H_{42}O_{15}Na]^+$: 845.2; found: 845.2. **^{1}H-NMR(400MHz, CDCl$_3$)** : 8.05 (d, H-Ph, $J = 7.2$ Hz), 7.91 (d, H-Ph, $J = 7.2$ Hz), 7.77 (d, H-Ph, $J = 3.2$ Hz), 7.60–7.10 (m, H-Ph), 6.1 (dd, 1H, H_4, $J_{4\text{-}5} = J_{4\text{-}3} = 10$ Hz), 5.87 (dd, 1H, H_3, $J_{3\text{-}2} = 1.6$Hz, $J_{3\text{-}4} = 9.6$ Hz), 5.83–5.74 (m, 1H, H_8), 5.67 (m, 1H, H_2), 5.30 (d, 1H, H_1, $J_{1\text{-}2} = 2$ Hz), 5.25 (dd, 1H, H_{9B}, $J_{9A\text{-}9B} = 1.6$Hz, $J_{trans} = 16.8$ Hz), 5.11 (dd, 1H, H_{9A}, $J_{cis} = 10.4$ Hz), 4.60 (dd, 1H, H_{6B}, $J_{gem} = 12$ Hz, $J_{6B\text{-}5} = 2$ Hz), 4.46 (dd, 1H, H_{6A}, $J_{6A\text{-}5} = 4.8$ Hz), 4.42–4.36 (m, 1H, H_5), 4.06–3.97 (m, 2H, D_2, H_{7B}), 3.88 (dd, 1H, H_{7A}, $J_{gem} = 12.8$Hz, $J_{7A\text{-}8} = 5.6$ Hz), 3.78 (bs, 1H, D_1), 3.05–2.95 (m, 2H, D_4, D_5), 2.21–2.09 (m, 2H, D_{6ax}, D_{3ax}), 2.05–1.89 (m, 2H, $D_{6eq}D_{3eq}$). **^{13}C-NMR(100 MHz, CDCl$_3$)**: 180.2, 179.9 (COOH); 166.2, 165.6, 165.5, 165.4 (CO_{BZ}); 134.5 (C_8); 133.5, 133.5, 133.2 (CH_{BZ}); 129.9, 129.9, 129.8, 129.8, 129.8, 129.0 (CH_{BZ}); 129.1, 129.1, 129.0, 128.9 (C_{quatBZ}); 128.6, 128.5, 128.5, 128.3, 128.3 (CH_{BZ}); 117.2 (C_9); 96.3 (C_1); 73.5 (C_{D1}); 72.7 (C_{D2}); 70.8 (C_2); 70.1 (C_7); 69.8 (C_5);

69.7 (C_3); 67.0 (C_4); 63.1 (C_6); 39.0, 39.2 (C_{D4}, C_{D5}); 27.4 (C_{D3}); 26.9 (C_{D6}).

*General procedure for the synthesis of anilides **44–50***

To a 0.6 M solution of the diacid **15** (1 eq.) in dry DMA, HATU (1.1 eq.) and the appropriate aniline (3 eq.) were added under stirring and under nitrogen atmosphere at room temperature. The reaction mixture was warmed to 50 °C. After disappearance of the starting material (TLC 9:1 $CHCl_3$:MeOH and 98:2 $CHCl_3$:acetone) another aliquot of HATU (1.1 eq.) and of aniline (3 eq.) was added under stirring. The reaction was stirred at 50 °C for 3 days. After reaction completion the solvent was evaporated at reduced pressure. The product was purified by membrane filtration using Isolute Phase Separator columns. Therefore, the crude reaction product was dissolved in CH_2Cl_2 (1 mL) and charged onto a column with 1M HCl (1 mL). The organic phase was eluted and charged onto another column containing 1M NaOH. The organic phase was dried over sodium sulphate and the solvent evaporated under reduced pressure. The crude was purified by flash chromatography (98:2 $CHCl_3$:MeOH) to yield anilides **37–43**, that were deprotected using the following procedure.

A 1 M solution of sodium methoxyde (2 eq.) in MeOH was added to a 0.05 M solution of the bis-anilide (1 eq.) in dry methanol under stirring and under nitrogen atmosphere at room temperature. After reaction completion (TLC 88:12 toluene:acetone) the reaction mixture was diluted with methanol and neutralized with pre-washed Amberlite IRA 120-H^+. The resin was filtered off and the solvent evaporated under reduced pressure. Crude anilides **44–50** were purified by flash chromatography (95:5 → 9:1 $CHCl_3$:MeOH).

Biological assay

Preparation and culture of dendritic cells

Buffy coats from the venous blood of normal healthy volunteers were obtained by the Blood Transfusion Centre of Slovenia, according to institutional guidelines. The study was approved by the National Medical Ethics Committee of the Ministry of Health, Republic of Slovenia, and written consent was obtained before collection of specimens.

Peripheral blood mononuclear cells were isolated using Lympholyte®-H (Cedarlane laboratories, Ontario, Canada). The cells were washed twice with Dulbecco's phosphate-buffered saline (DPBS), counted, and used as the source for immunomagnetic isolation of CD14-positive cells (Miltenyi Biotec GmbH, Bergisch Gladbach, Germany). These were cultured in RPMI 1640 (Cambrex) medium supplemented with 10% fetal bovine serum (FBS), gentamicin (50 μg/mL; Gibco, Paisley, UK), 500 U/mL of rhGM-CSF and 400 U/mL of rhIL-4 (both Gentaur, Paris, France). On day 2, half of the medium was exchanged with starting quantities of rhGM-CSF (500 U/mL) and rhIL-4 (400 U/mL). After 5 days, non-adherent, immature DCs were harvested and characterized by flow cytometry as $CD1a^{hi}$, $CD83^{-}$, $CD86^{low}$ and $HLA^{-}DR^{low}$ (data not shown). Cells were counted and re-suspended in the medium containing 500 U/mL of rhGM-CSF and 20 ng/mL LPS, and cultured for a further 2 days [33].

Measurement of dendritic cell adhesion with CFSE fluorescence assay

Wells of a 96-well culture plate (Nunc Nunclon Δ surface or Nunc MaxiSorp) were precoated with 50 μL of mannan (1.0 mg/mL) (Sigma) in carbonate buffer, pH 9.6, overnight at 4°C. Wells were then washed once with PBS and incubated with 1% BSA in PBS for 30 min at room temperature. Various volumes of 50 mM of stock solution of ligands were added to the wells to obtain the required final concentrations in the assay. PBS or DMSO was used in controls. Immature DCs were harvested, washed with PBS and labelled with 2.5 μM carboxyfluorescein succinimidyl ester (CFSE) according to the manufacturer's protocol (Molecular Probes, Invitrogen, Eugene, USA) [34], and re-suspended in the medium containing 500 U/mL of rhGM-CSF and either rhIL-4 (1000 U/mL) or 20 ng/mL LPS at concentration 5×10^5/mL. 50 μL of this immature DC suspension was then added to wells and the cells were allowed to attach for 90 min. Wells were then washed twice with PBS, and 50 μL of lysis buffer (25 mM Tris, 0.1% SDS) was added. Each experiment was done in quadruplicate for each concentration of antagonist used and for control cells. To estimate the total immature DCs added to wells, one quadruplicate of wells was not washed with PBS, but only lysis buffer was added directly. CFSE is colourless and non-fluorescent until the acetate groups are cleaved by intracellular esterases to yield highly fluorescent carboxyfluorescein succinimidyl ester which reacts with intracellular amines, forming fluorescent conjugates. The fluorescence was measured at 520 ± 10 nm with a Tecan Saphire microplate reader (Tecan Group, Maennedorf, Switzerland, excitation wavelength 490 nm) and is directly proportional to the number of adhered cells. Cell adherence was determined by Eq. 1, where A_{tx} and $A_{totalDC}$ are the fluorescence of CFSE determined for cells washed after different times and for all dendritic cells. A_{blank} is the background fluorescence of the buffer.

$$\text{Cell adherence } (\%) = (A_{tx} - A_{blank}/A_{total\ DC} - A_{blank}) \times 100. \quad (1)$$

The IC_{50} values were calculated by fitting mean values of DC-SIGN-mediated cell adherence versus log (antagonist concentration) to the logistic (sigmoid) equation by non-linear least-squares curve-fitting using OriginPro 7.5 and 8

software [35]. All the experimental data are presented with standard error bars. Control experiments were performed for known DC-SIGN antagonists **1** and **2**, and two DC-SIGN specific antibodies (H200 and 1B10) in order to prove DC-SIGN specific inhibition.

Results and discussion

Structure-based design of substituted 1,2-mannobioside mimics

HIV-1, *M. tuberculosis* [7] and a number of other pathogens including viruses (HIV-1, HCV, CMV, Dengue, Ebola, SARS-CoV, HSV, coronaviruses, H5N1, West Nile virus, measles virus) and bacteria (*Helicobacter pylori* and *Leptospira interrogans*) [36–44] bind to DC-SIGN through mannosylated glycoproteins (gp120 and ManLAM). To improve the binding affinity of mannose-based glycoconjugates, we have explored the known crystal structure of DC-SIGN carbohydrate-recognition domain (CRD) in complex with tetramannoside Man_4 (PDB code: 1SL4) [26] in search for binding sites on DC-SIGN CRD whose binding potential is not entirely exploited by the mimics designed so far [11–16,21]. The primary interaction of the oligosaccharide occurs by coordination of the non-reducing end residue of the oligosaccharide to a Ca^{2+} binding site exposed on the surface of the protein (shown as blue sphere, Fig. 3) [24]. Examination of this crystal structure allows identification of two structural features of DC-SIGN CRD as favourable sites to increase overall free energy of binding. A hydrophobic region defined by the phenyl ring of Phe 313 (Fig. 3) interacts weakly with the Man2 residue of Man_4. It has been postulated that Phe 313 plays a double role in the binding mode of branched mannosides: it increases affinity (albeit weakly) by forming part of a surface complementary to the shape of Manα1-6Man moiety of Man_4, and it allows access to the α-linked outer arm branch trimannose structure while preventing binding of β-linked mannosides and *N*-linked glycans that have only the core branch trimannose structure [24]. Man3 residue does not interact with the receptor at all, but rather it points away from the protein and allows binding of high-mannose oligosaccharides. The hydrophobic cavity/area behind Phe313 (Fig. 3) is also a likely interaction region, which does not make any contact with the Man3 residue.

Based on these observations, we have sought to modify the structure of the pseudo-disaccharide **1** (Fig. 4) to include fragments capable of interacting with one, or possibly both, proposed binding sites. The interaction of **1** and DC-SIGN was studied by NMR spectroscopy [12], suggesting that the ligand should anchor to DC-SIGN CRD through complexation of the Ca^{2+} binding site by its mannose residue. Indeed, preliminary docking studies confirmed this hypothesis and suggested that the cyclohexane ring of **1** may extend towards the Phe 313 region in the protein binding site. Hence, additional lipophilic fragments could be added to the framework of **1** exploiting the carboxy groups appended to the cyclohexane ring (Fig. 4). Identification of hydrophobic contacts in the proximity of the binding site of oligosaccharides and addition of lipophilic fragments to a sugar 'core' have often been applied to improve the affinity of glycomimetics [11,45–49].

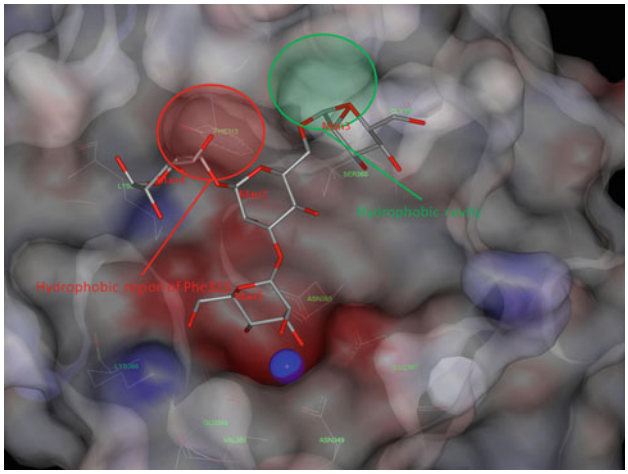

Fig. 3 Crystal structure of DC-SIGN CRD (shown as solvent-accessible surface) in complex with Man_4 (shown as tubes) with proposed binding regions unoccupied by Man_4. Mannose residues and important amino acid residues for Man_4 binding are labelled as *ovals*, Ca^{2+} coordinated by Man1 residue is presented as a sphere

The docking model used did not have the predictivity required to allow selection of the amide residues by virtual screening. A small library of substituted aromatic and non-aromatic derivatives of general structure **4** was therefore prepared (Fig. 4 and Table 1) looking for initial Structure-Activity Relationship (SAR) data. Preliminary SPR studies [50] showed that tertiary amides had no affinity for DC-SIGN, so mostly secondary amides were synthesized and only one tertiary amide (compound **28**, Table 1) was tested in the present study.

The synthetic approach used is shown in Scheme 1. Two different condensation strategies were employed to synthesize amides or anilides from the preformed pseudo-disaccharides **13** and **15**, respectively. These in turn were obtained by appropriate modification of the sequence previously described for the synthesis of **1,** starting from enantiomerically pure acid **5** [32]. For the synthesis of amides **26–36**, pentafluorophenyl esters could be used as protecting groups of the carboxylic acids in the first four steps and then exploited as activated esters for the reaction of intermediate **13** with the appropriate amines. Thus, the di-PFPester **6** was treated with MCPBA to give epoxide **8**, which was

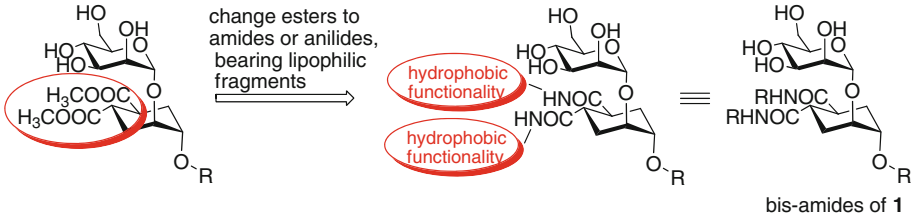

Fig. 4 The design of novel substituted 1,2-mannobioside mimics and general structure of the bis-amide derivatives of **1**

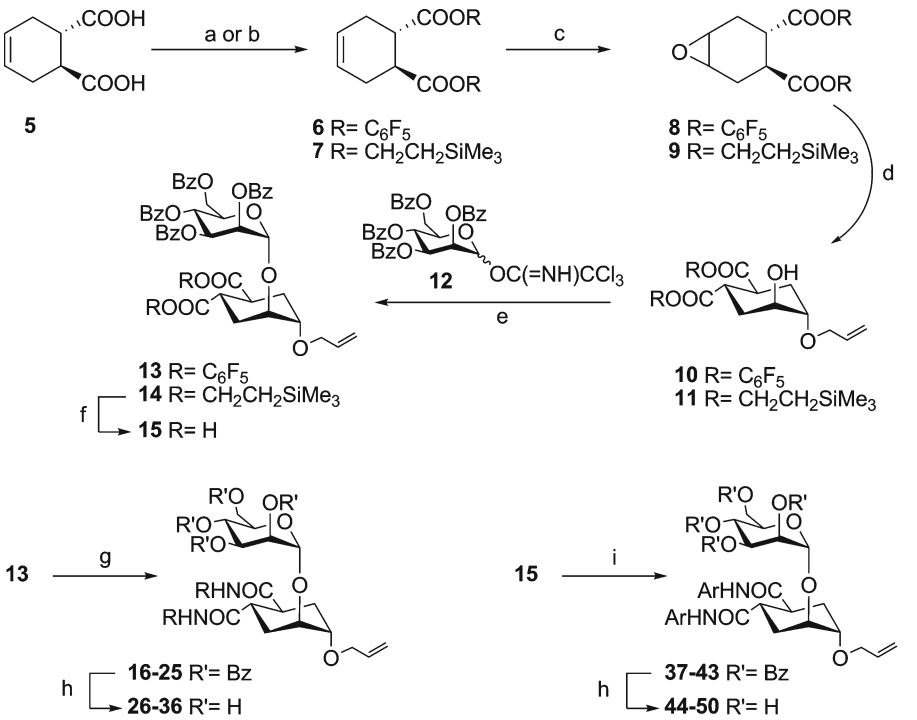

Scheme 1 Synthetic scheme leading to amides **26–36** and to anilides **44–50**. The structure of the R groups is shown in Table 1

a) EDC, C_6F_5OH, THF (6, 88%); b) DCC, DMAP, $Me_3SiCH_2CH_2OH$ (7, 86%); c) MCPBA, CH_2Cl_2 (8, 78%; 9, 71%); d) $Cu(OTf)_2$, allyl alcohol (10, 95%; 11, 91%); e) 12, TMSOTf, 0.2 eq, CH_2Cl_2, -20°C (13, 56%; 14, 48%); f) 1:1 CF_3COOH : CH_2Cl_2, R.T., 100%; g) 2.4 eq RNH_2, THF, 20 h; h) MeONa, MeOH; i) excess $ArNH_2$, HATU, DMA.

opened with allylic alcohol under copper (II) triflate catalysis in almost quantitative yields. The resulting alcohol **10** was mannosylated with trichloroacetimidate **12** to give **13**. This sequence afforded the scaffold **13** in four steps starting from diacid **5** with 37% overall yield. Treatment of **13** with 2.4 mol/equiv of the required amine in THF overnight afforded amides **16–25**. The crude compounds after Isolute HM-N work-up (see experimental) were directly deprotected under Zemplen's conditions to afford amides **26–36** (Note: amide **35** was obtained by NaOH hydrolysis of the tetra-*O*-benzoate **24**).

Under the same conditions, reaction of **13** with aniline afforded 39% of mono-anilide products, along with 30% of recovered starting material. Thus, a different strategy was implemented for the synthesis of anilides **44–50**, starting from the trimethylsilylethyl ester **7** (Scheme 1). This was elaborated as described above to afford the corresponding pseudo-disaccharide **14**. Ester deprotection with trifluoroacetic acid in CH_2Cl_2 [51] afforded acid **15** which was transformed in anilides **37–43** by reaction with an excess of the appropriate aniline and 2 mol/equiv of *O*-(7-azabenzotriazole)-*N,N,N′,N′*-tetramethyluronium hexafluorophosphate (HATU) [52,53] following a carefully devised addition protocol (see experimental). The crude compounds after membrane filtration work-up (see experimental) were chromatographed and deprotected under Zemplen's conditions to afford anilides **44–50.**

Biological assay and interpretation of the results

The activity of ligand candidates was tested using an assay we recently described [25] which measures the ability of molecules to inhibit dendritic cells adhesion to mannan-coated

Table 2 IC_{50} of DC-SIGN specific antibodies (H200, 1B10), reference compound **2**, and compounds **26–33** and **44–47** in the DC adhesion test

Compound	IC_{50}	R^2
H200	6.095 ± 1.040 μg/mL	0.966
1B10	1.454 ± 0.651 μg/mL	0.967
2	299 ± 30.0 μM	0.994
26	344 ± 10.4 μM	0.999
27	339 ± 7.69 μM	0.982
28	6.86 ± 0.24 μM[a]	0.988
29	29.5 ± 2.28 μM	0.995
30	90.0 ± 1.87 μM	0.967
31	44.2 ± 13.2 μM	0.986
33	12.8 ± 3.42 μM	0.982
44	12.5 ± 3.90 μM	0.989
45	26.6 ± 0.72 μM	0.999
46	45.8 ± 9.3 μM	0.980
47	111 ± 2.10 μM	0.971

[a]Maximal inhibition observed for compound **28** was 54% (46% adhesion)

plates (see experimental for details). To assess whether this assay identifies inhibitors of DC-SIGN-mediated adhesion, adhesion was measured in the presence of different concentrations of DC-SIGN specific antibodies, 1B10 and H200, and their IC_{50} values were determined (Table 2) [54,55]. The results demonstrate that DC adhesion to the mannan-coated plate can be abolished by DC-SIGN specific antibodies (Supplementary data) and an IC_{50} of 6.1 + 1.0 μg/mL and 1.4 + 0.6 μg/mL was determined for the two antibodies, respectively. In the presence of 1B10, a monoclonal blocking antibody, maximum inhibition of DC adhesion was high (up to 80%), confirming that the assay detects DC-SIGN specific antagonists. H200 is a polyclonal blocking antibodies directed against DC-SIGN neck region (amino acids 61–200) rather than its CRD. Likely this antibody, which only allows maximum inhibition ca. 65%, reduces DC-SIGN-mediated adhesion by steric interference to the mannan-coated surface. It should be noted that neither antibody allowed to achieve 100% inhibition of adhesion [25]. This suggests that DC adhesion to mannan-coated plates does not rely solely on DC–SIGN, but also exploits other DC expressed mannose-binding receptors [56]. Nonetheless, the assay can serve as a preliminary screening for binding inhibitor candidates. Furthermore, compounds **1** and **2** were used as a positive control and **2** was found to inhibit DC adhesion with IC_{50} = 299 ± 30.0 μM (Table 2), which corresponds well to the IC_{50} obtained by SPR (IC_{50}(**2**) = 125 μM) [21].

Preliminary single-point tests were used to identify candidates for IC_{50} measurement. All synthesized compounds were tested in concentration 0.5 mM to assess their inhibition on immature dendritic cell adhesion (Fig. 5). The compounds

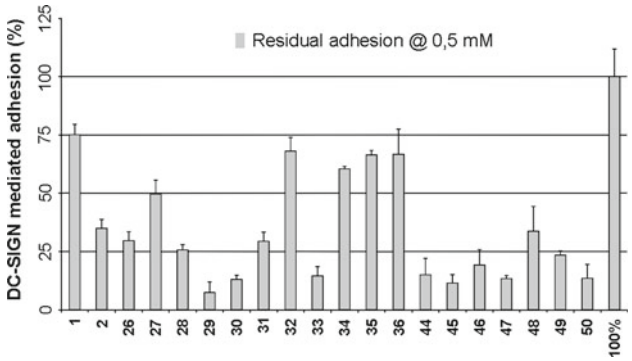

Fig. 5 Single-point test for compounds **26–36** and **44–50** showing residual adhesion at 0.5 mM with reference compounds **1** (X = N_3) and **2**

that exhibited at least 50% inhibition of cell adhesion (50% of residual adhesion) at 0.5 mM concentration were tested for dose-response and their IC_{50} values were determined. Based on this cut-off value, compounds **32** and **34–36** were not chosen for IC_{50} determination. In addition, compounds **48–50** precipitated in the preliminary test (apparent on visual inspection), so these compounds were excluded from further testing.

IC_{50} values were determined for compounds **26–31**, **33** and **44–47** (Table 2). The original binding data are reported as Supplementary Information. The highest inhibitory potency was observed for compound **28**, although maximal inhibition observed for this compound was only 54% (46% adhesion). Similar, albeit slightly less potent, inhibition was observed for compounds **29**, **31**, **33** and **44–46**. The results strongly indicate that the majority of the substituents selected were reasonable and have increased potency as DC-SIGN antagonists when compared to starting compound **1**, which inhibited DC adhesion only weakly (Fig. 5). Some ligands were also found to be more potent than the pseudo-trisaccharide **2**, up to 1 order of magnitude. Since amide **29** bears simple benzyl moieties and compounds **44–46** carry phenyl or 4-tolyl lipophilic groups (Table 1), we conclude that simple aromatic rings with or without small substituents are optimal for strong interaction with DC-SIGN. This strongly suggests that additional binding affinity to DC-SIGN may be attributed primarily to hydrophobic interactions and confirms our preliminary hypothesis. The assay used in this article [25] measures the influence of the antagonists on binding of DC to mannan-coated plates. Since immature dendritic cells can express various mannose binding lectins [56] it is difficult to distinguish the contributions of the different lectins to the adhesion process. However, the ability of the DC-SIGN specific antibody 1B10 to reduce adhesion by 80% suggests that DC-SIGN is a major determinant of the binding ability to mannan-coated plates, and therefore, the assay can serve as a preliminary screening. The most interesting candidates iden-

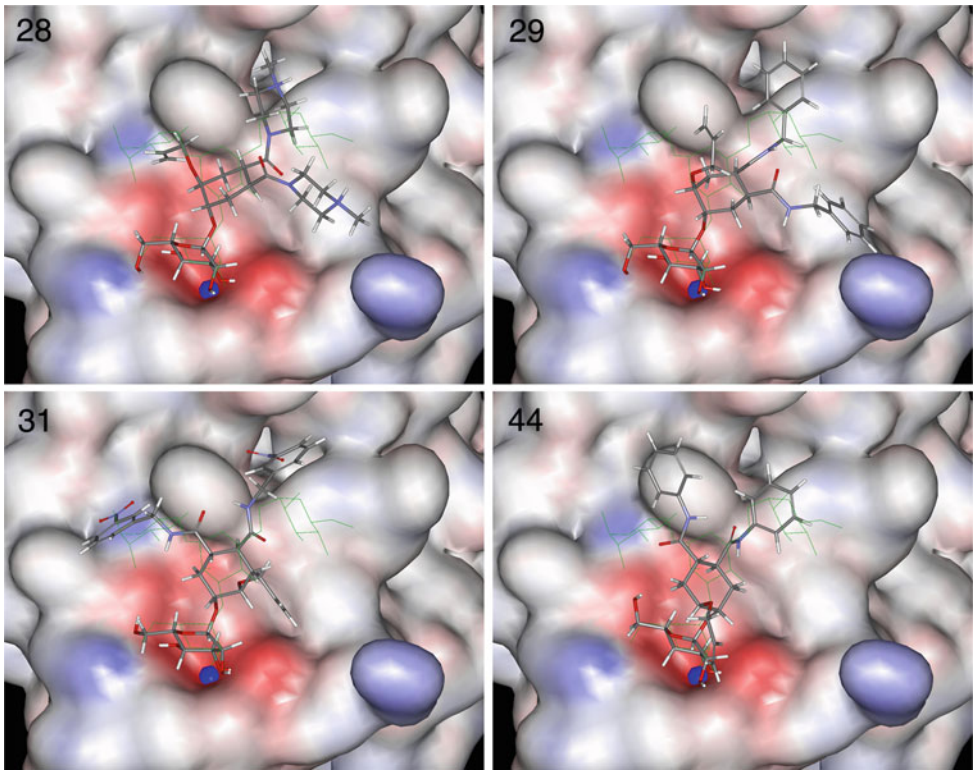

Fig. 6 Crystal structure of DC-SIGN CRD (shown as solvent–accessible surface; Ca^{2+} coordinated by Man1 residue is presented as a sphere) in complex with Man_4 (shown as lines) and top docked poses of compounds **28**, **29**, **31** and **44** (shown as tubes)

tified by this approach will be further examined for activity and specificity using assays based on isolated DC-SIGN [15,19].

Proposed binding modes of the synthesized mannose-based DC-SIGN antagonists

The expected binding mode of **28**, **29**, **31** and **44** as predicted with FlexX molecular docking tool is shown in Fig. 6. Similar poses were obtained for all the other ligands analyzed, but no strong quantitative correlation was found between the calculated scores and the experimental inhibitory concentration. The conformations proposed by the FlexX show a markedly consistent binding mode for the mannose residue of all docked compounds identical to the Man1 residue in the crystal structure of DC-SIGN CRD (1SL4). Apart from Man1 residue, FlexX predicted two principal binding modes of the diamide part of the molecules:

- The first binding mode is depicted for compounds **28** and **29** (Fig. 6), where lipophilic residues stretch towards the hydrophobic cavity behind Phe 313 and the other points to the Arg345 residue (aminoacid residue at the right bottom of the figures, Fig. 6),
- The second binding mode is depicted for compounds **31** and **44**, where both lipophilic residues 'embrace' Phe 313.

Both predicted binding modes include interaction with at least one of the targeted lipophilic sites and could explain increased affinity to DC-SIGN. Furthermore, the predicted binding modes indicate that further improvement in binding affinity might be obtained by exploiting additional interactions, for instance with Arg345 guanidine.

Conclusion

In the search for potent monovalent DC-SIGN antagonists, we have taken advantage of the known crystal structure of DC-SIGN CRD in complex with Man_4 tetramannoside (1SL4). After a careful examination of the DC-SIGN binding site, we identified two regions only partially exploited by native ligands which could be used to increase the potency of glycomimetic DC-SIGN antagonists. Upon this hypothesis, we designed and synthesized a small focused library of mannose glycoconjugate derivatives of the previously published DC-SIGN antagonist **1**. The compounds were tested using a DC adhesion assay to mannan-coated plates and the results demonstrate that the majority of the new derivatives inhibit DC adhesion more potently, by up to 2 orders of magnitude, than the starting compound **1**. Additionally, docking studies allowed qualitative rationalization of the results and suggested that the synthesized DC-SIGN antagonists occupy one or both predicted binding sites.

Acknowledgments This study was supported by a grant from the Research Agency of the Republic of Slovenia (grant P1-0208 to MA and P4-0127 to NO), by the Women in Science UNESCO award (NO) and by the Italian FIRB program CHEM-PROFARMANET—(RBPR05NWWC). Mass spectra were obtained through the Centro Interdipartimentale Grandi Apparecchiature (CIGA) at the University of Milan. The authors thank Dr. Roger Pain for careful reading of the manuscript and many useful suggestions.

References

1. Steinman RM, Banchereau R (2007) Taking dendritic cells into medicine. Nature 449:419–426. doi:10.1038/nature06175
2. Gringhuis SI, den Dunnen J, Litjens M, van Het Hof B, van Kooyk Y, Geijtenbeek TB (2007) C-Type lectin DC-SIGN modulates toll-like receptor signaling via Raf-1 kinase-dependent acetylation of transcription factor NF-κB. Immunity 26:605–616. doi:10.1016/j.immuni.2007.03.012
3. Geijtenbeek TB, den Dunnen J, Gringhuis SI (2009) Pathogen recognition by DC-SIGN shapes adaptive immunity. Futur Microbiol 4:879–890. doi:10.2217/fmb.09.51
4. Gringhuis SI, den Dunnen J, Litjens M, van der Vlist M, Geijtenbeek TB (2009) Carbohydrate-specific signaling through the DC-SIGN signalosome tailors immunity to *Mycobacterium tuberculosis*, HIV-1 and *Helicobacter pylori*. Nat Immunol 10:1081–1088. doi:10.1038/ni.1778
5. Švajger U, Anderluh M, Jeras M, Obermajer N (2010) C-type lectin DC-SIGN; an adhesion, signalling and antigen-uptake molecule that guides dendritic cells in immunity. Cell Signal 22:1397–1405. doi:10.1016/j.cellsig.2010.03.018
6. Coutanceau E, Decalf J, Martino A, Babon A, Winter N, Cole ST, Albert ML, Demangel C (2007) Selective suppression of dendritic cell functions by *Mycobacterium ulcerans* toxin mycolactone. J Exp Med 204:1395–1403. doi:10.1084/jem.20070234
7. van Kooyk Y, Appelmelk B, Geijtenbeek TBH (2003) A fatal attraction: *Mycobacterium tuberculosis* and HIV-1 target DC-SIGN to escape immune surveillance. Trends Mol Med 9:153–159. doi:10.1016/S1471-4914(03)00027-3
8. Geijtenbeek TB, Kwon DS, Torensma R, van Vliet SJ, van Duijnhoven GC, Middel J, Cornelissen IL, Nottet HS, Kewal-Ramani VN, Littman DR, Figdor CG, van Kooyk Y (2000) DC-SIGN, a dendritic cell-specific HIV-1-binding protein that enhances transinfection of T cells. Cell 100:587–597. doi:10.1016/S0092-8674(00)80694-7
9. van Kooyk Y, Geijtenbeek TBH (2003) DC-SIGN: escape mechanism for pathogens. Nat Rev Immunol 3:697–709. doi:10.1038/nri1182
10. Khoo US, Chan KYK, Chan VSF, Lin CLS (2008) DC-SIGN and L-SIGN: the SIGNs for infection. J Mol Med 86:861–874. doi:10.1007/s00109-008-0350-2
11. Ernst B, Magnani JL (2009) From carbohydrate leads to glycomimetic drugs. Nat Rev Drug Discov 8:661–677. doi:10.1038/nrd2852
12. Reina JJ, Sattin S, Invernizzi D, Mari S, Martinez-Prats L, Tabarani G, Fieschi F, Delgado R, Nieto PM, Rojo J, Bernardi A (2007) 1,2-Mannobioside mimic: synthesis, DC-SIGN interaction by NMR and docking, and antiviral activity. ChemMedChem 2:1030–1036. doi:10.1002/cmdc.200700047
13. Borrok MJ, Kiessling LL (2007) Non-carbohydrate inhibitors of the lectin DC-SIGN. J Am Chem Soc 129:12780–12785. doi:10.1021/ja072944v
14. Mitchell DA, Jones NA, Hunter SJ, Cook JMD, Jenkinson SF, Wormald MR, Dwek RA, Fleet GWJ (2007) Synthesis of 2-C-branched derivatives of D-mannose: 2-C-aminomethyl-D-mannose binds to the human C-type lectin DC-SIGN with affinity greater than an order of magnitude compared to that of D-mannose. Tetrahedron 18:1502–1510. doi:10.1016/j.tetasy.2007.06.003
15. Timpano G, Tabarani G, Anderluh M, Invernizzi D, Vasile F, Potenza D, Nieto PM, Rojo J, Fieschi F, Bernardi A (2008) Synthesis of novel DC-SIGN ligands with an α-fucosylamide anchor. ChemBioChem 9:1921–1930. doi:10.1002/cbic.200800139
16. Garber KCA, Wangkanont K, Carlson EE, Kiessling LL (2010) A general glycomimetic strategy yields non-carbohydrate inhibitors of DC-SIGN. Chem Commun 46:6747–6749. doi:10.1039/C0CC00830C
17. Rojo J, Delgado R (2004) Glycodendritic structures: promising new antiviral drugs. J Antimicrob Chemother 54:579–581. doi:10.1093/jac/dkh399
18. Lasala F, Arce E, Otero J, Rojo F, Delgado R (2003) Mannosyl glycodendritic structures inhibit DC-SIGN-mediated ebola virus infection in *cis* and in *trans*. Antimicrob Agents Chemother 47:3970–3972. doi:10.1128/AAC.47.12.3970-3972.2003
19. Tabarani G, Reina JJ, Ebel C, Vives C, Lortat-Jacob H, Rojo F, Fieschi F (2006) Mannose hyperbranched dendritic polymers interact with clustered organization of DC-SIGN and inhibit gp120 binding. FEBS Lett 580:2402–2408. doi:10.1016/j.febslet.2006.03.061
20. Wang S-K, Liang P-H, Astronomo RD, Hsu TL, Hsieh S-L, Burton DR, Wong C-H (2008) Targeting the carbohydrates on HIV-1: interaction of oligomannose dendrons with human monoclonal antibody 2G12 and DC-SIGN. Proc Natl Acad Sci USA 105:3690–3695. doi:10.1073/pnas.0712326105
21. Sattin S, Daghetti A, Thépaut M, Berzi A, Sánchez-Navarro M, Tabarani G, Rojo J, Fieschi F, Clerici M, Bernardi A (2010) Inhibition of DC-SIGN-mediated HIV infection by a linear trimannoside mimic in a tetravalent presentation. ACS Chem Biol 5:301–312. doi:10.1021/cb900216e
22. Martìnez-Avila O, Bedoya LM, Marradi M, Clavel C, Alcamì J, Penadés S (2009) Multivalent manno-glyconanoparticles inhibit DC-SIGN-mediated HIV-1 trans-infection of human T cells. ChemBioChem 10:1806–1809. doi:10.1002/cbic.200900294
23. Martìnez-Avila O, Hijazi K, Marradi M, Clavel C, Campion C, Kelly C, Penadés S (2009) Gold manno-glyconanoparticles: multivalent systems to block HIV-1 gp120 binding to the lectin DC-SIGN. Chem Eur J 15:9874–9888. doi:10.1002/chem.200900923
24. Guo Y, Feinberg H, Conroy E, Mitchell DA, Alvarez R, Blixt O, Taylor ME, Weis WI, Drickamer K (2004) Structural basis for distinct ligand-binding and targeting properties of the receptors DC-SIGN and DC-SIGNR. Nat Struct Mol Biol 11:591–598. doi:10.1038/nsmb784
25. Obermajer N, Švajger U, Jeras M, Sattin S, Bernardi A, Anderluh M (2010) An assay for functional DC-SIGN inhibitors of human dendritic cell adhesion. Anal Biochem 406:222–229. doi:10.1016/j.ab.2010.07.018
26. CambridgeSoft©. ChemBioOffice Ultra, ChemBioDraw version 12.0.
27. CambridgeSoft©. ChemBioOffice Ultra, ChemBio3D Ultra version 12.0, GAMESS interface.
28. Crystal Structure of DC-SIGN carbohydrate recognition domain complexed with Man_4. Protein data bank. http://www.pdb.org/pdb/explore/explore.do?structureId=1SL4. (Accessed 6 July 2009)
29. BioSolve IT (GmbH). FlexX version 3.1.2.
30. Accelrys Software Inc.© Discovery Studio v 2.5.5.9350.
31. Lee DJ, Kowalczyk R, Muir VJ, Rendle PM, Brimble MA (2007) A comparative study of different glycosylation methods for the synthesis of D-mannopyranosides of *N*-_-fluorenylmethoxycarbonyl-trans-4-hydroxy-L-proline allyl ester. Carbohydr Res 342:2628–2634. doi:10.1016/j.carres.2007.08.015

32. Bernardi A, Arosio D, Manzoni L, Micheli F, Pasquarello A, Seneci P (2001) Stereoselective synthesis of conformationally constrained cyclohexanediols: a set of molecular scaffolds for the synthesis of glycomimetics. J Org Chem 66:6209–6216. doi:10.1021/jo015570b
33. Švajger U, Vidmar A, Jeras M (2008) Niflumic acid renders dendritic cells tolerogenic and up-regulates inhibitory molecules ILT3 and ILT4. Int Immunopharmacol 8:997–1005. doi:10.1016/j.intimp.2008.03.006
34. Molecular ProbesTM, Invitrogen detection technologies: CellTraceTM CFSE Cell Proliferation Kit (C34554), Product information. Revised 24-June-2005 [Online]. http://probes.invitrogen.com/media/pis/mp34554.pdf. (Accessed 26 August 2009)
35. OriginLab©. Data Analysis and Graphing Software. OriginPro version 7.5 and 8.
36. Klimstra WB, Nangle EM, Smith MS, Yurochko AD, Ryman KD (2003) DC-SIGN and L-SIGN can act as attachment receptors for alphaviruses and distinguish between mosquito cell- and mammalian cell-derived viruses. J Virol 77:12022–12032. doi:10.1128/JVI.77.22.12022-12032.2003
37. Lozach PY, Lortat-Jacob H, de Lacroix de Lavalette A, Staropoli I, Foung S, Amara A et al (2003) DC-SIGN and L-SIGN are high affinity binding receptors for hepatitis C virus glycoprotein E2. J Biol Chem 278:20358–20366. doi:10.1074/jbc.M301284200
38. Tassaneetrithep B, Burgess TH, Granelli-Piperno A, Trumpfheller C, Finke J, Sun W et al (2003) DC-SIGN (CD209) mediates dengue virus infection of human dendritic cells. J Exp Med 197:823–829. doi:10.1084/jem.20021840
39. Lin G, Simmons G, Pohlmann S, Baribaud F, Ni H, Leslie GJ et al (2003) Differential N-linked glycosylation of human immunodeficiency virus and Ebola virus envelope glycoproteins modulates interactions with DC-SIGN and DC-SIGNR. J Virol 77:1337–1346. doi:10.1128/JVI.77.2.1337-1346.2003
40. Marzi A, Gramberg T, Simmons G, Moller P, Rennekamp AJ, Krumbiegel M et al (2004) DC-SIGN and DC-SIGNR interact with the glycoprotein of Marburg virus and the S protein of severe acute respiratory syndrome coronavirus. J Virol 78:12090–12095. doi:10.1128/JVI.78.21.12090-12095.2004
41. Yang ZY, Huang Y, Ganesh L, Leung K, Kong WP, Schwartz O et al (2004) pH-Dependent entry of severe acute respiratory syndrome coronavirus is mediated by the spike glycoprotein and enhanced by dendritic cell transfer through DC-SIGN. J Virol 78:5642–5650. doi:10.1128/JVI.78.11.5642-5650.2004
42. Regan AD, Whittaker GR (2008) Utilization of DC-SIGN for entry of feline coronaviruses into host cells. J Virol 82:11992–11996. doi:10.1128/JVI.01094-08
43. Wang SF, Huang JC, Lee YM, Liu SJ, Chan YJ, Chau YP et al (2008) DC-SIGN mediates avian H5N1 influenza virus infection in *cis* and in *trans*. Biochem Biophys Res Commun 373:561–566. doi:10.1016/j.bbrc.2008.06.078
44. Gaudart N, Ekpo P, Pattanapanyasat K, van Kooyk Y, Engering A (2008) *Leptospira interrogans* is recognized through DC-SIGN and induces maturation and cytokine production by human dendritic cells. FEMS Immunol Med Microbiol 53:359–367. doi:10.1111/j.1574-695X.2008.00437.x
45. Bernardi A, Cheshev P (2008) Interfering with the sugar code: design and synthesis of oligosaccharide mimics. Chem Eur J 14:7434–7441. doi:10.1002/chem.200800597
46. Cumpstey I, Salomonsson E, Sundin A, Leffler H, Nilsson UJ (2008) Double affinity amplification of galectin–ligand interactions through arginine–arene interactions: synthetic, thermodynamic, and computational studies with aromatic diamido thiodigalactosides. Chem Eur J 14:4233–4245. doi:10.1002/chem.200701932
47. Tejler J, Salameh B, Leffler H, Nilsson UJ (2009) Fragment-based development of triazole-substituted *O*-galactosyl aldoximes with fragment-induced affinity and selectivity for galectin-3. Org Biomol Chem 7:3982–3990. doi:10.1039/B909091F
48. Mesch S, Lemme K, Koliwer-Brandl H, Strasser DS, Schwardt O, Kelm S, Ernst B (2010) Kinetic and thermodynamic properties of MAG antagonists. Carbohydr Res 345:1348–1359. doi:10.1016/j.carres.2010.03.010
49. Mesch S, Moser D, Strasser DS, Kelm A, Cutting B, Rossato G, Vedani A, Koliwer-Brandl H, Wittwer M, Rabbani S, Schwardt O, Kelm S, Ernst B (2010) Low molecular weight antagonists of the myelin-associated glycoprotein: synthesis, docking, and biological evaluation. J Med Chem 53:1597–1615. doi:10.1021/jm901517k
50. Sattin S (2009) Synthesis of Inhibitors of DC-SIGN mediated infections. Ph.D. Thesis, University of Milan.
51. Sanchez-Navarro M (2009) Sintesis de sistemas multivalentes de carbohidratos basados en glicodendrones. Ph.D. Thesis, University of Seville.
52. Carpino LA (1993) 1-Hydroxy-7-azabenzotriazole. An efficient peptide coupling additive. J Am Chem Soc 115:4397–4398. doi:10.1021/ja00063a082
53. Ye Y, Liu J, Kao MLK, Marshall GR (2003) Peptide-bond modification for metal coordination: peptides containing two hydroxamate groups. Pept Sci 71:489–515. doi:10.1002/bip.10471
54. Hodges A, Sharrocks K, Edelmann M, Baban D, Moris A, Schwartz O, Drakesmith H, Davies K, Kessler B, McMichael A, Simmons A (2007) Activation of the lectin DC-SIGN induces an immature dendritic cell phenotype triggering Rho-GTPase activity required for HIV-1 replication. Nature Immun 8:569–577. doi:10.1038/ni1470
55. Tailleux L, Schwartz O, Herrmann JL, Pivert E, Jackson M, Amara A, Legres L, Dreher D, Nicod LP, Gluckman JC, Lagrange PH, Gicquel B, Neyrolles O (2003) DC-SIGN is the major *Mycobacterium tuberculosis* receptor on human dendritic cells. J Exp Med 197:121–127. doi:10.1084/jem.20021468
56. Turville SG, Cameron PU, Handley A, Lin G, Pöhlmann S, Doms RW, Cunningham AL (2002) Diversity of receptors binding HIV on dendritic cell subsets. Nat Immunol 3:975–983. doi:10.1038/ni841